



AKADÉMIAI KIADÓ

Comparison of different preparation methods for oxygen isotope determination of phosphate in mammal tooth enamel


Central European
Geology

65 (2022) 2, 144–157

DOI:

[10.1556/24.2023.00132](https://doi.org/10.1556/24.2023.00132)

© 2023 The Author(s)

GABRIELLA ILONA KISS^{1,2*} , PÉTER SZABÓ³,
MARIANNA TÚRI¹, ISTVÁN FUTÓ¹, JÁNOS KOVÁCS³ and
LÁSZLÓ PALCSU¹

¹ Isotope Climatology and Environmental Research Centre, HUN-REN Institute for Nuclear Research, Debrecen, Hungary

² Doctoral School of Physics, University of Debrecen, Debrecen, Hungary

³ Institute of Geography and Earth Sciences, University of Pécs, Pécs, Hungary

Received: August 19, 2022 • Accepted: August 16, 2023

Published online: September 27, 2023

RESEARCH ARTICLE



ABSTRACT

We tested several sample pre-treatment protocols for the study of oxygen isotope ratios in the phosphate phase of mammalian enamel of ten different fossil samples. We investigated the effect of different pre-treatment methods and the duration of the hydrogen fluoride treatment on enamel samples from skeletal phosphate with known $\delta^{18}\text{O}$ values. The samples had been measured previously, so we could compare the ratios measured in our laboratory with the previous values to choose the best chemical preparation procedure. Four pre-soaking methods and two different time intervals of 2 mol dm^{-3} hydrogen fluoride treatment were compared during our experiments. In our experimental conditions, the distilled water wash and the 6 h of soaking in hydrogen fluoride gave the closest results to the expected δ -values. The steps of the tested preparation processes were repeated at least three times on each sample, so the reproducibility of the process could be also investigated.

KEYWORDS

bioapatite, fossil mammal teeth, oxygen isotopes, paleoclimate reconstruction, phosphate, pre-treatment protocols

INTRODUCTION

Nowadays, it is increasingly important to obtain more information about past climate conditions. Knowing more details about the climatic parameters results in a deeper understanding of the drivers and mechanisms of climate changes in the past; more precise modelling of the ongoing and future processes can be performed. The oxygen isotope composition in the water cycle is very well known and widely used in hydrologic as well in paleoclimate studies. The oxygen isotope ratio of different compounds (such as ice, groundwater, carbonate, bone, tree ring, or sphagnum) have a huge importance in understanding climate proxy data (White et al., 2004; Steiger et al., 2017; Kock et al., 2019; Xu et al., 2021).

The relationship between the oxygen isotope composition of local precipitation and ambient temperature is widely known and used for climate reconstruction (Dansgaard, 1964). The oxygen isotope composition in skeletal material of mammals is mainly affected by their water intake from food and drinking water, both of which are determined by the local oxygen isotope composition of the environmental water. The body temperature of mammals is quite constant and regulated by their metabolism (Longinelli, 1984; Luz et al., 1984);

*Corresponding author. Isotope Climatology and Environmental Research Centre, Institute for Nuclear Research, Bem tér 18/C, H-4026 Debrecen, Hungary.
E-mail: kiss.gabriella@atomki.hu

thus, isotope fractionation during other processes, such as the oxygen composition of inhaled air, humidity, sweat, or urine are independent of climate or negligible, and contribute to the equilibrium oxygen-isotope composition in the body to a lesser extent (Gehler et al., 2011). From all these factors, the ingested environmental water plays the most significant role in the water–tissue oxygen-equilibrium process in the body of the terrestrial mammal. Due to the correlation between isotopic composition of the oxygen-bearing materials (e.g., enamel from teeth) and isotopic composition of the environmental water as well as local temperature, the oxygen isotopic investigation of terrestrial mammal fossils can contribute to an understanding of the climatic conditions in the past.

Bones and teeth have a high percentage of inorganic compounds. The chemical composition of the most important inorganic compound, the so-called biogenic hydroxylapatite or bioapatite (Pasero, et al., 2010), is expressed with the following basic molecular formula: $\text{Ca}_{10}(\text{PO}_4)_6(\text{OH}, \text{CO}_3)_2$. Beside the phosphate, the other oxygen-containing groups are the carbonate and hydroxide groups. As the phosphate ions have a higher abundance compared to structural carbonates, the PO_4^{3-} groups can be considered as the main source of oxygen in the hardest tissues, such as enamel from teeth (Chenery et al., 2012). Secondary carbonate is another source of carbonate. This is another type of carbonate mineral (calcite, dolomite) that may attached to fossil vertebrate remains. The removal of secondary carbonate is a critical point during the preparation, especially in the case of structural carbonate $\delta^{13}\text{C}$ and $\delta^{18}\text{O}$ measurements. Compared to the carbonate isotope analysis from bioapatite, the isotope analysis of the phosphate content seems easier, possibly due to the robustness of the PO_4^- group. There is a strong chemical bond between oxygen and phosphorus atoms in the phosphate group, where breaking a single covalent bond has an activation energy of 350 kJ mol^{-1} . This makes chemical changes and/or isotope exchange processes at low temperatures unlikely, but does not make the structure resistant enough to microbiological activity or phosphatase enzyme activity, except for enamel, which has a better-crystallized structure and a moderate pore size distribution (Blake et al., 1997; Sharp et al., 2000; Zazzo et al., 2004). Compared to bones, tooth enamel is a much more robust material, and these effects are less important in this case. The crystallite size of bioapatite from enamel is larger and they have lower carbonate (~3.5%; Kohn and Cerling, 2002; Wopenka and Pasteris, 2005), and only a small organic content (under 1% by volume; Olszta et al., 2007). The partial replacement of OH^- by F^- ions also results in a more robust material compared to bones, from a thermodynamical consideration (Keenan, 2016). However, after burial during early diagenesis, the loss of organic material from the structure allows fluids to infiltrate into the pores of the biomineral and also facilitates the incorporation of F^- , Cl^- , or CO_3^{2-} in place of OH^- or PO_4^{3-} ions (Chenery et al., 2012; Kohn and Cerling, 2002). In the case of bones, the total phosphorus concentration and environmental pH

can affect the structure and stability of the biomineral (Agnini et al., 2009). Also, the organic content (between 0.5 and 20%, depending on the section of the tooth) is lower in teeth compared to bones, where organic content is ~30% in living animals, but its degradation rate after death depends not only on time but also on the temperature and pH of the environment (Collins et al., 2002; Keenan, 2016; Olszta et al., 2007; Snoeck and Pellegrini, 2015).

Phosphate oxygen, especially in materials with relatively high crystallinity such as lamellar hydroxyfluorapatite, is also diagenetically more robust than the oxygen in the carbonate or hydroxyl group of bioapatite (Kohn et al., 1999; Puc at et al., 2010). As a result, for fossil mammal remains, the tooth enamel is the best component to use for stable isotope study for tracing in-vivo environmental conditions (Iacumin et al., 1996). The crystallites in the teeth are larger and well-ordered and contain less carbonate and more fluoride than the crystallites in bones (Wopenka and Pasteris, 2005; Keenan, 2016; Kocsis, 2011).

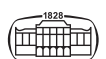
Oxygen isotope ratio values are expressed in δ -values, based on the $^{18}\text{O}/^{16}\text{O}$ isotope ratio of the sample (R_{sample}) and the isotope ratio of a standard material (R_{standard}), given in equation (1) below. The result is quoted in permil (‰).

$$\delta^{18}\text{O} = (R_{\text{sample}}/R_{\text{standard}} - 1) \times 1000\text{‰} \quad (1)$$

This $\delta^{18}\text{O}$ value is different in the environmental water ($\delta^{18}\text{O}_{\text{W}}$) than that of the biogenic phosphate ($\delta^{18}\text{O}_{\text{PO}_4}$) due to fractionation during incorporation into the tissues, but this relationship can be described as a linear function (Longinelli, 1984; Luz et al., 1984; Kohn and Cerling, 2002; Iacumin et al., 1996; Luz and Kolodny, 1985; Iacumin and Venturelli, 2015). Thus, past temperature over the last few hundred thousand or even millions of years can be reconstructed from the oxygen isotopic composition of bioapatite of mammal tissue fossils (Iacumin et al., 1996).

Since the relationship between the isotope composition of environmental water and the ambient temperature is also linear (Craig, 1961; Dansgaard, 1964; Rozanski, 1993; Vodila et al., 2011), the oxygen isotope composition of the phosphate in bioapatite must reflect the temperature of the local environment. This fractionation is well described not only for a few species of animals, but also for humans (Longinelli, 1984; Luz et al., 1984).

For accurate determination of oxygen isotope composition, beside the precise measurement, applying of an adequate preparation protocol is essential. Different laboratories have their own different protocols, so in this study, our goal was to develop our own procedure, based on mammal teeth, which can be followed in the case of phosphate oxygen isotope determination, in accordance with the other measurement protocols we apply on similar hard-tissue samples. In the case of the carbonate content of bioapatite, a few sample preparation studies are available (Snoeck and Pellegrini, 2015; Garvie-Lok et al., 2004; Pellegrini and Snoeck, 2016), where hydrogen peroxide in different concentrations, sodium hypochlorite and hydrazine hydrate were investigated as pre-cleaning agents. The researchers here found that sodium hypochlorite was the



most effective against organic contaminants, but in using this chemical, some altering effects on the carbon and oxygen isotope ratios were observed, due to precipitation of artificial carbonate. However, some protocols follow up the sodium hypochlorite with a (Ca-buffered) acetic acid solution that may help mitigate the negative effects of the bleach. Hydrogen peroxide seemed less effective in the case of removal of organic materials. Hydrazine hydrate was considered an applicable chemical agent, but because of its physiological effects, in our laboratory, we did not prefer its application.

The sensitivity of chemical procedures to the isotopic composition of the phosphate content has also been studied in recent years. There are many different procedures given in the literature, not only in relation to pre-cleaning, but also for the acidic treatment as well. Thus, we decided to compare the most commonly used traditional methods on samples with a well-known oxygen isotope ratio, to adopt an efficient and precise protocol. These traditional methods contain – after several cleaning steps in order to get rid of the contamination – the precipitation step with silver nitrate solution. Those studies use different cleaning agents: the most frequently used chemicals are sodium hypochlorite, hydrogen peroxide (in different concentrations) or both of them combined with an acetate buffer solution or simply acetic acid, in different concentrations and reaction time (Chenery et al., 2012; Lécuyer et al., 1993; Vennemann et al., 2002). However, during sediment phosphate isotope analyses, sodium hydrogen carbonate, sodium hydroxide and hydrochloric acid were also investigated as pre-treating chemicals (Liu et al., 2019). Other studies apply diluted nitric acid (0.5 mol dm^{-3}) to dissolve the phosphate content

from the samples, but in this case, the minimum time requirement of the reaction may be quite long, up to several days (LaPorte et al., 2009). Some references mention the possibility of a very gentle pre-cleaning, or not carrying out any pre-cleaning steps at all, but this approach is recommended mostly in case of dental enamel powders (Zazzo et al., 2004; Grimes and Pellegrini, 2013; Szabó et al., 2017). Figure 1 shows what can be measured from bioapatite, what are the key points in the case of preparation for oxygen stable isotope measurements, and some references which are also mentioned and cited elsewhere in the text and the reference list.

Recent studies show that cation and anion exchange chromatography is also a highly applicable tool for separation of the phosphate content, applied in conjunction with the silver phosphate precipitation method (LaPorte et al., 2009; Pederzani et al., 2020). However, in many cases, the effect of these chemicals upon the measured isotope composition of the phosphate is not negligible (Grimes and Pellegrini, 2013). Based on those, we attempted to choose the most effective method, in order to clean our samples not only from the organic residues but also the inorganic oxygen-containing groups, especially secondary carbonates. The chosen samples for testing our preparation protocol were tooth enamel from *Stephanorhinus* sp. (two-horned rhinoceros), *Rhinocerotidae* sp. (rhinoceros) and *Mammuthus* sp. (mammoth), as is presented in Table 1 below. The samples were retrieved from different geographical locations, which are also indicated in Table 1. The sample selection is based not only on the sufficient sample amount but also on the widest possible range of the previously known $\delta^{18}\text{O}$ values.

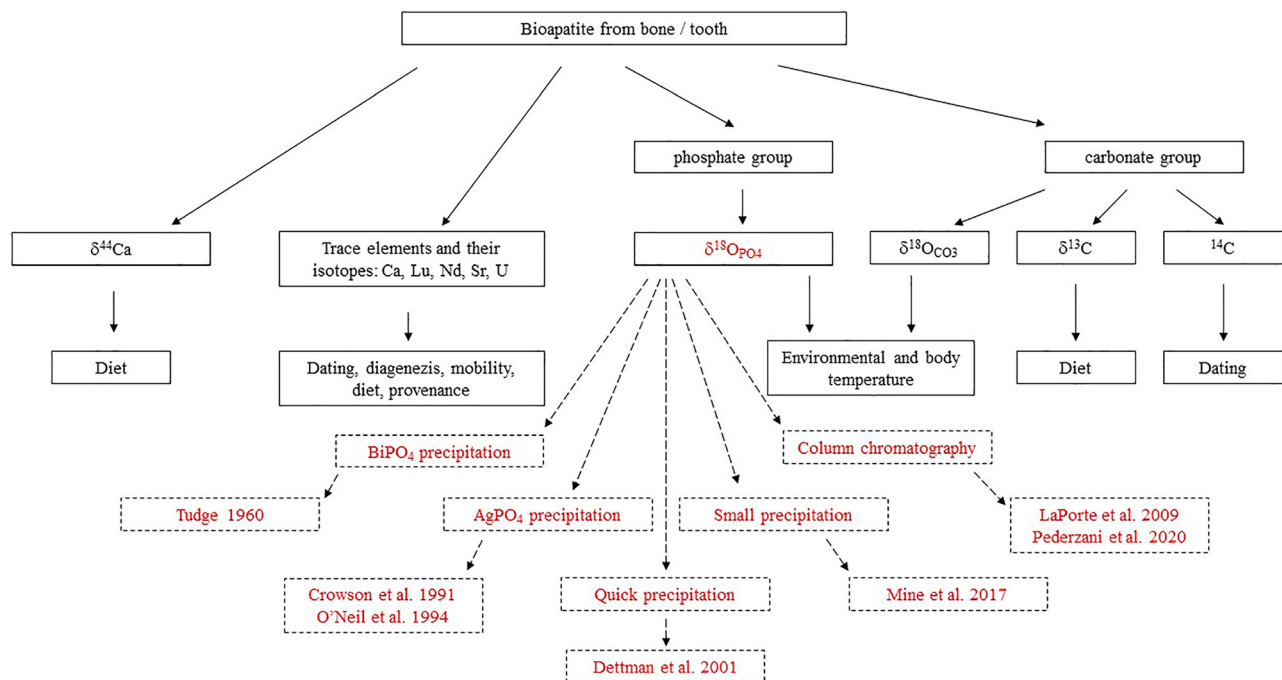


Fig. 1. Summary of the measurement opportunities from bioapatite, including the main approaches of phosphate separation/precipitation and the most important references (written red) (Crowson et al., 1991; Dettman et al., 2001; LaPorte et al., 2009; Mine et al., 2017; O'Neil et al., 1994; Pederzani et al., 2020)



As is listed in Table 1 below, the location of the samples are Italy, France, Slovakia, and Hungary. From Italy, the collected samples are derived from the *Stephanorhinus* species. The age of the samples was between ~5.2 Ma and ~1 Ma (Szabó et al., 2017), based on classification into mammalian biozones. The samples collected in France are members of different mammal species: *Anancus arvernesis*, *Stephanorhinus* sp. and *Mammuthus meridionalis* (southern mammoth). The determined ages of the samples are between 2.47 Ma and 1.8 Ma (Szabó et al., 2017; Boivin et al., 2010). One sample was collected in Slovakia; this is a *Stephanorhinus jeanvireti* species, the age of which is between 2.6 Ma and 1.9 Ma. Also, from the Carpathian Basin, in Hungary, three samples were collected: a *Stephanorhinus* sp. from Pécel and a *Mammuth borsoni* from Százhalombatta; their ages are between 3.5 Ma and 1.9 Ma. The third Hungarian sample is a *Rhinocerotidae* indet., collected in Rudabánya, and is determined as a sample from the Miocene (Szabó et al., 2017).

MATERIALS AND METHODS

Pre-treatment and digestion methods were compared on tooth samples with a known oxygen isotope composition to improve our method for precise preparation, measurement, and calibration. The preparation methods were tested on enamel samples of teeth collected in North Italy, France, Slovakia, and Hungary, with previously-published $\delta^{18}\text{O}_{\text{phosphate}}$ vs. V-SMOW values between +11‰ and +20‰ (Szabó et al., 2017). The samples were previously measured at the University of Lausanne, where a DeltaPlus XL mass spectrometer connected with a TC/EA high-temperature elemental analyzer and a Conflo interface was the measuring instrument (Vennemann et al., 2002). The measured values were calculated against two in-house standards (LK-2L, $\delta^{18}\text{O} = +12.1\text{‰} \pm 0.3\text{‰}$ and LK-3L, $\delta^{18}\text{O} = +17.9\text{‰} \pm 0.3\text{‰}$). In our experiments, the samples for the preparation tests were chosen based on their previous $\delta^{18}\text{O}$ results: our goal was to cover as wide range as possible, in terms of oxygen isotope values.

The preparation steps for the measurement series consisted of a pre-cleaning step using different chemicals (distilled water, calcium-acetate–acetic acid buffer solution, and/or hydrogen peroxide or sodium hypochlorite solution). For dissolving the phosphate content of the samples, hydrogen fluoride solution was applied. During our experiments, the effect of the different pre-cleaning methods and the duration of the HF treatment (6 and 24 h) were examined in order to determine the effects of different chemical agents and the duration of the acid treatment on the dissolution of the bioapatite. Before the chemical preparation of bioapatite, the first step is sampling from the chosen teeth. After mechanical cleaning – in order to get rid of the impurities from the surrounding soil residues and other visible contaminants – and slicing, a few mg powder (under 125 μm particle size) was collected from each tooth enamel with a diamond-tipped Dremel[®] 3,000 drilling/grinding

machine. Where it was possible, the samples were collected from the crown to the root, along the entire length of each tooth.

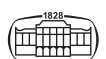
After sample collection, the preparation consisted of two more steps. In the second step, we attempted to remove all possible organic residues (which can build up between the apatite crystals and on their surface) and secondary carbonates from the sample. In the literature, distilled water, calcium-acetate–acetic acid buffer, hydrogen peroxide, and sodium hypochlorite are the most common chemical agents, although – against its hazardous properties – some studies suggest using hydrazine hydrate. Here we note that publications point to the avoidance of cleaning steps where possible (Kocsis, 2011; Grimes and Pellegrini, 2013; Szabó et al., 2017). The third part of the procedure was the dissolution of the phosphate content of the samples, using HF. Here, the concentration of the solution and the duration of the treatment can also affect the isotopic composition (Grimes and Pellegrini, 2013; Lécuyer, 2004). The final goal was to eliminate any other oxygen-containing groups e.g., CO_3^{2-} , OH^- , organics, and transfer PO_4^{3-} into Ag_3PO_4 , which is a good alternative to the previously used BiPO_4 (Longinelli, 1984; Kohn and Cerling, 2002; Luz and Kolodny, 1985; Lécuyer, 2004; Tudge, 1960). The oxygen isotope composition of the bioapatite phosphate was measured in the form of a silver phosphate precipitate. During the preparation, single-use plastic tubes (volume: 2.0 ml) from Eppendorf[®], single-use needles, and syringes were used. All the chemicals used were analytical reagent grade. Each sample was prepared in triplicate.

Pre-cleaning methods

In the first step of the preparation, 5 mg of each pulverized sample was placed in a vessel and soaked in the chosen solution based on the processes in Table 2. The first batch of samples was only immersed in distilled water at room temperature for 6 h. In the second attempt, after gently rinsing with distilled water, the samples were stored in an acetic acid–Ca-acetate buffer (1 mol dm^{-3}) for another 6 h. These samples were then rinsed with distilled water twice, centrifuged (13,000 rpm, 3 min), and dried at 60 °C to constant weight. Their mass was measured after drying. The 3rd set of samples was soaked in 10 w% H_2O_2 solution for 24 h; after this step, they were rinsed with distilled water three times. Following this step, 1.5 ml 1 mol dm^{-3} calcium acetate–acetic acid buffer solution was applied for another 6 h. The 4th sample set was treated with sodium hypochlorite solution (10–12 w%, 24 h), rinsed at least three times with distilled water, and soaked in calcium acetate–acetic acid buffer solution for another 6 h. After the pre-cleaning, the samples were washed with distilled water and then dried at 60 °C till constant weight.

Phosphate extraction and measurement

The residues were then dissolved in 800 μl hydrofluoric acid (2 mol dm^{-3}). These samples were then centrifuged, the supernatant fluid (above the calcium fluoride precipitate)



was transferred to clean vials, and a few drops of NH_4OH (25 w%) was added to each sample to reach neutral pH, which was determined using pH paper (interval: pH 1–12).

After that, AgNO_3 solution (500 μL , 2 mol dm^{-3}) was added to each sample to precipitate silver phosphate. After 30 min, the russet precipitate was centrifuged and washed with distilled water three times and centrifuged (13,000 rpm, 3 min). The samples were dried at 60 °C until constant weight, and then 0.3 mg from each sample was placed in a silver capsule for stable isotope analysis. The samples in the silver capsules were kept in a desiccator to avoid the effect of adsorption of the humidity from the ambient atmosphere.

The samples were measured in the Isotope Climatology and Environmental Research Centre, Institute for Nuclear Research (Debrecen, Hungary), on a Thermo Finnigan DeltaPlus XP continuous flow isotope ratio mass spectrometer, connected with a TC/EA high-temperature elemental analyzer using a zero-blank autosampler. The oxygen isotopic analysis using TC/EA is based on the high-temperature conversion of Ag_3PO_4 on glassy carbon to carbon monoxide. The reduction temperature was 1,450 °C. Before the mass spectrometric analysis, the resulting components (CO and residual gases) are separated on a gas chromatography column. During the continuous flow measurement, the sample provides a transient signal, and pulses of the reference gas are injected. Two different reference materials were used for the calculations. The first was an Elemental Microanalysis measurement standard (B2207, $\delta^{18}\text{O}$ vs. V-SMOV = +21.7‰ \pm 0.3‰), and the second was an in-house silver phosphate powder with $\delta^{18}\text{O}$ value of +12.26‰ \pm 0.3‰, determined at the University of Lausanne against USGS-80 ($\delta^{18}\text{O}$ = +12.5‰ \pm 0.18‰) and USGS-81 reference materials ($\delta^{18}\text{O}$ = +34.7‰ \pm 0.19‰). The preparation steps were carried out by all the samples at least three times, and each prepared sub-sample was measured three times. Our standard deviation in the case of oxygen isotope ratio measurements is 0.3‰ (1 σ).

RESULTS AND DISCUSSION

Pre-cleaning methods

We tested several pre-cleaning methods to remove organic compounds and secondary carbonates. To evaluate the effect of the chemical treatments the following statistical indicators are applied for comparison of the results in the case of each method:

- ΣD^2 : the sum of the squares of the absolute differences between the measured and the nominal $\delta^{18}\text{O}$ results;
- $\Sigma(D^2 \times s^2)$: sum of the squares of the absolute differences multiplied by the square of the standard deviation (s).

A chemical yield has been calculated as the ratio of the final mass of the silver phosphate and the mass of the pre-cleaned bioapatite sample, and then compared to the theoretical value. Figures 2C, F, 3C and F show the chemical yields in percentages. Most of them are between 60 and 80%,

which can be acceptable. The presence of biocarbonate, as well as the loss of phosphate precipitate (due to transferring and rinsing the solutions), can lower the chemical yield. As we described earlier, every sample was prepared three times, and those sub-samples were measured by the mass spectrometer three times. Therefore, the given averages and standard deviations were calculated using those nine values in the case of each sample.

No extra pre-cleaning (NE). Some of the literature (Bergmann et al., 2018) suggest no pre-cleaning or washing procedure is necessary; the only cleaning is done with water, so we built this step into the experiments. After the water treatment, no significant mass decrease could be observed as shown in Figs 2B and C. The average remainder of 99.4% of the original sample amount could indicate that during the cleaning step a relatively low amount of surface contamination was removed. However, in some cases, even an increase in mass was observed. As the measured weights of the samples were constant, we could exclude the possibility of an incomplete drying procedure. We suggest that any increase in mass is caused by the adsorption of moisture from the air, even though the samples were stored in a desiccator. In this case of this method, the measured oxygen isotope values were closer to the known ratios than in our other experiments, within a 1.5‰ difference compared to the known data (see Tables 1 and 2 in Appendix and Fig. 2A). For the NE methods, the ΣD^2 and the $\Sigma(D^2 \times s^2)$ are the lowest among all methods, indicating the best agreement with the standard data.

Acetate buffer only (A). Acetate buffering was used in the next three pre-cleaning experiments. When using acetate buffer only, the samples were soaked in 1.5 mL 1 mol dm^{-3} Ca-acetate–acetic acid buffer solution for 6 h at room temperature. We found that mass reduction was observable in the case of using acetic acid buffer only: after pre-cleaning, 82.2 and 90.6% of the original material remained in the vials (see Tables 3 and 4 in Appendix and Fig. 2E), as was already observed in case of the structural carbonate content of bioapatite samples (Snoeck and Pellegrini, 2015). The measured values were quite close to the known ones compared to the nominal data. The values of ΣD^2 (8.27 and 8.71) and $\Sigma D^2 \times s^2$ (0.19 and 1.38) indicate that our results agreed well with the nominal δ -values, with a maximum difference of 1.52‰ (see Appendix Tables 3 and 4) and similar to the NE results. The CO chromatography peak areas here were in agreement with those from the applied standard materials (mentioned in Section 2.2.).

Hydrogen peroxide and acetate buffer solution (PA). Some references suggest using hydrogen peroxide in its concentrated form (~30 w%), but in many cases, the diluted solution was tested as a cleaning agent at this step of the protocol, and in some cases, higher temperatures were also applied for this solution. However, during some



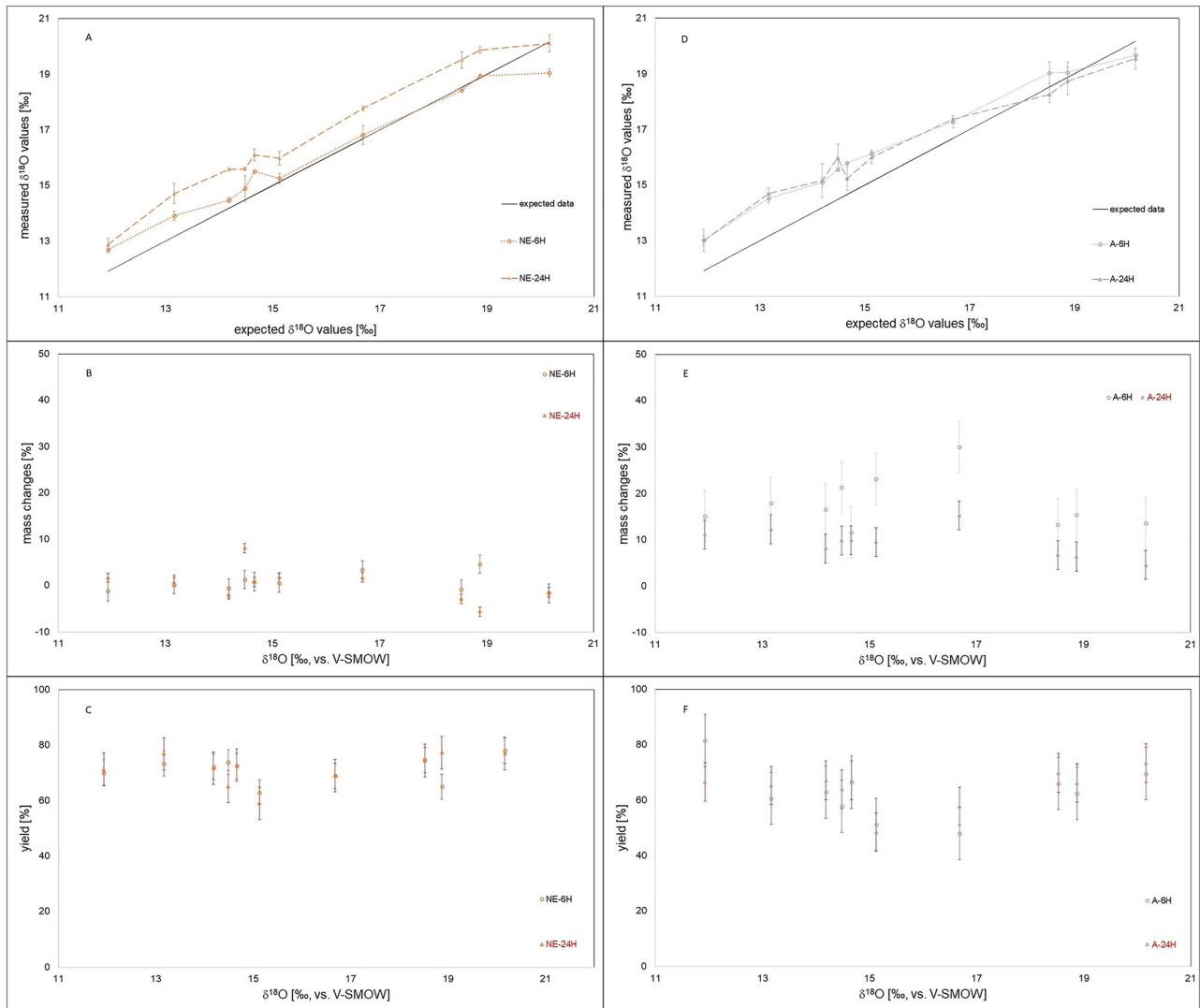


Fig. 2. The measured $\delta^{18}\text{O}$ values (A, D), mass changes after the pre-cleaning steps (the difference between the initial mass and the measured mass after the pre-cleaning; hence, if the mass change is positive, there is some mass loss) (B, E), and the calculated yield of the preparation processes (C, F) in case of the NE (A, B, C) and A (D, E, F) series

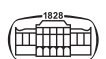
experiments, the alteration of the original isotope signature and organic residues was observed when using H_2O_2 solution in its higher concentrated forms (Grimes and Pellegrini, 2013). In the current study, we decided to use 10 w% H_2O_2 and room temperature incubation for 24 h.

The change in mass before and after preparation was moderate using hydrogen peroxide and acetate buffer for the preparation steps (see Fig. 3B). The average sample residues were 81.9% and 86.0% of the original samples, which are similar to the A method. In contrast, the measured isotope showed a greater difference compared to the previous data, with a maximum difference of 2.70‰ in the case of the PA-6H batch and 2.36‰ in the case of the PA-24H series (see Appendix Tables 5 and 6). This indicates that some fractionation occurred during this preparation process, in good agreement with earlier publications in this field (Grimes and Pellegrini, 2013). The

statistical indicators were higher than in previous cases: for ΣD^2 28.21 and 20.41 were given, and for $\Sigma(D^2 \times s^2)$ 9.86 and 4.22 were calculated. Also, the peak areas were about 25% smaller than the results of the measured standard materials, indicating some dissolution of the phosphate and other compounds, as was already observed elsewhere (Grimes and Pellegrini, 2013; Snoeck and Pellegrini, 2015; Pellegrini and Snoeck, 2016).

Sodium Hypochlorite and Acetate buffer solution (HCA).

Here, we observed the largest mass loss during the preparation, the sodium hypochlorite solution digested more than 30% of the samples on average over 24 h, causing the largest differences in $\delta^{18}\text{O}$ based on the calculated statistical values (ΣD^2 : 29.97 and 11.01, $\Sigma(D^2 \times s^2)$: 12.82 and 4.29), especially for the HCA-6H series (2.55‰, see Appendix Tables 7 and 8) which showed the greatest deviation from



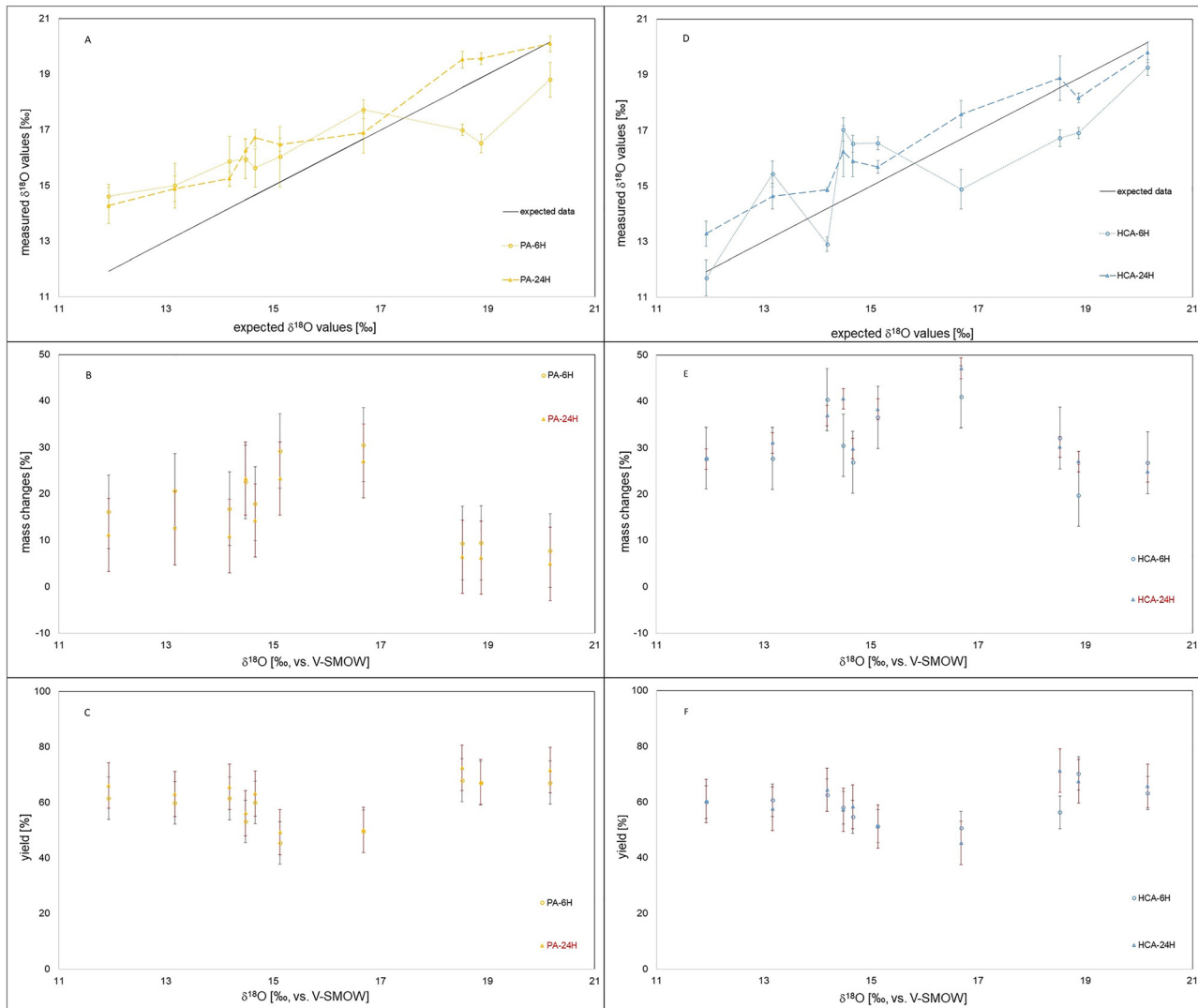


Fig. 3. The measured $\delta^{18}\text{O}$ values (A, D), the mass changes after the pre-cleaning steps (the difference between the initial mass and the measured mass after the pre-cleaning; hence, if the mass change is positive, there is some mass loss) (B, E), and the calculated yield of the preparation processes (C, F) in the case of the PA (A, B, C) and HCA (D, E, F) series

the expected δ -values. Previous tests on bioapatite with HCA confirmed that not only the organic materials but also the inorganic parts including bioapatite were digested. However, in the case of using lower concentrations, or shorter dissolution time, the mass loss can be less significant; nevertheless, we avoided using sodium hypochlorite in further preparations.

Time dependence of the hydrogen fluoride treatment

Differences in the acidic treatment time intervals are mentioned in the literature (Grimes and Pellegrini, 2013; Kocsis, 2011). Here, we investigated two-time intervals: first, the samples were soaked in 2 mol dm^{-3} HF for 6 h, and in the second experiment series, the duration was 24 h. In the case of chemical pre-cleaning experiments (A-, PA- and HCA-experiments) not only the isotope ratio data (Figs 4A

and 4B) but also the measured peak areas showed differences compared to standard silver phosphate salts. After 6 h of acid treatment, the carbon monoxide peak areas released from the samples were smaller than the peaks during the measurement of the reference materials, especially in the case of the last two methods (PA, HCA), while after the 24-h treatment, the peak areas were similar to the peaks from the reference materials. This was in good agreement with the previous protocols established in many laboratories (Zazzo et al., 2004; Grimes and Pellegrini, 2013; Lécuyer, 2004; Lécuyer et al., 2019). Based on these results, we can conclude that a longer acidic treatment is necessary to completely dissolve the teeth, so 24 h is a preferred time interval. However, in the case of the gentler NE experiment (no extra pre-cleaning), the 6-h HF digestion gave slightly better results than the 24-h digestion, although the difference of goodness is not significant.



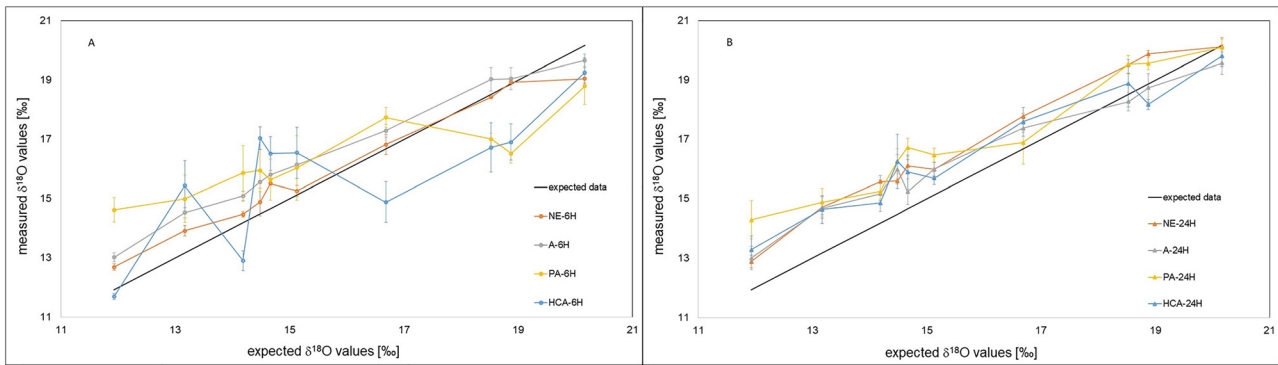


Fig. 4. Comparison of the effect of the different pre-cleaning methods on the measured oxygen isotope results in the case of 6 h (A) and 24 h (B) acidic treatment

CONCLUSIONS

We have investigated the isotopic changes in the phosphate phase of several teeth samples, compared to the previously measured isotopic composition of the same samples, and assessed the effects of the pre-cleaning and the HF treatment. During the experiments, four different pre-cleaning processes were examined, from which distilled water as pre-cleaning material was found to ensure the closest results to the previously measured values. We also found that a 6-h acid treatment to dissolve the phosphate gave the closest values when soaking in distilled water was used as a pre-cleaning procedure. For the calibration of the mass spectrometric analysis, one in-house standard and one commercial reference material were used. Based on these experiments and measured results, we have selected the distilled water and 6-h long acidic treatment with 2 mol dm⁻³ hydrogen fluoride solution (NE-6H) method as the most suitable preparation in case of our sample series, under our laboratory circumstances. For future analysis, we recommend the final recipe as shown here:

1. The samples in powder form (drilled and pulverized in agate mortar) are kept in distilled water for 6 h and then dried to constant weight.
2. The preferred time of the acid treatment with 2 mol dm⁻³ hydrogen fluoride is 6 h. After the HF, the pH of the samples is suggested to set pH $\sim 7 \pm 1$ by using 25 w% NH₄OH added drop by drop, and the Ag₃PO₄ can be precipitated with 2 mol dm⁻³ silver nitrate solution. After washing and drying the precipitate, the samples can be placed into silver capsules for measurement.

Although this study confirms previous observations and the suggested recipe is suitable for mammal bioapatite samples, when selecting the best preparation process, first the sample material must be thoroughly examined in terms of organic content, secondary carbonate, apatite-associated carbonate, mineral structure, etc. Based on our experimental work and measured results, with the properly chosen recipe, isotope fractionation during the cleaning and preparation can be avoided. Besides its simplicity, the other important

advantage of our method is that this is financially more affordable than other protocols, using ion exchange resins. This, together with the correct calibration of the measurement (using in-house laboratory standards, if necessary), is a very useful and applicable tool for the precise determination of $\delta^{18}\text{O}$ values from the phosphate phase of fossil teeth. Due to the role of $\delta^{18}\text{O}_{\text{PO}_4}$ as a climate proxy, we have the opportunity to obtain more accurate information about the climate conditions and mammal behaviors from the past.

Funding: This work was supported by the European Union and the State of Hungary, co-financed by the European Regional Development Fund in the project of GINOP-2.3.2-15-2016-00009 'ICER'. This research was funded by NRDI Fund, grant number 2020-4.1.1-TKP2020.

Data availability statement: Data is contained within the article or supplementary material.

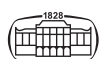
Conflicts of interest: The authors declare no conflict of interest.

ACKNOWLEDGMENTS

The English proofreading of Prof. Timothy Jull is highly appreciated.

REFERENCES

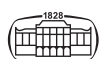
- Agnini, C., Macri, P., Backman, J., Brinkhuis, H., Fornaciari, E., Giusberti, L., Luciani, V., Rio, D., Sluijs, A., and Speranza, F. (2009). An early Eocene carbon cycle perturbation at ~ 52.5 Ma in the Southern Alps: chronology and biotic response. *Paleoceanography*, 24: 1–14. <https://doi.org/10.1029/2008PA001649>.
- Bergmann, K.D., Finnegan, S., Creel, R., Eiler, J.M., Hughes, N.C., Popov, L.E., and Fischer, W.W. (2018). A paired apatite and calcite clumped isotope thermometry approach to estimating Cambro-Ordovician seawater temperatures and isotopic



- composition. *Geochimica et Cosmochimica Acta*, 224: 18–41. <https://doi.org/10.1016/j.gca.2017.11.015>.
- Blake, R.E., O'Neil, J.R., and Garcia, G.A. (1997). Oxygen isotope systematics of biologically mediated reactions of phosphate: I. Microbial degradation of organophosphorus compounds. *Geochimica et Cosmochimica Acta*, 61: 4411–4422. [https://doi.org/10.1016/S0016-7037\(97\)00272-X](https://doi.org/10.1016/S0016-7037(97)00272-X).
- Boivin, P., Barbet, P., Boeuf, O., Devouard, B., Besson, J.C., Hénot, J.M., Devidal, J.L., Constantin, C., and Charles, L. (2010). Geological setting of the lower Pleistocene fossil deposits of Chillac (Haute-Loire, France). *Quaternary International*, 223–224: 107–115. <https://doi.org/10.1016/j.quaint.2009.12.010>.
- Chenery, C.A., Pashley, V., Lamb, A.L., Sloane, H.J., and Evans, J.A. (2012). The oxygen isotope relationship between the phosphate and structural carbonate fractions of human bioapatite. *Rapid Communications in Mass Spectrometry*, 26: 309–319. <https://doi.org/10.1002/rcm.5331>.
- Collins, M.J., Nielsen-Marsh, C.M., Hiller, J., Smith, C.I., Roberts, J.P., Prigodich, R. V., Wess, T.J., Csapò, J., Millard, A.R., and Turner-Walker, G. (2002). The survival of organic matter in bone: a review. *Archaeometry*, 44: 383–394. <https://doi.org/10.1111/1475-4754.t01-1-00071>.
- Craig, H. (1961). Isotopic variations in meteoric waters. *Science*, 133: 1702–1703. <https://doi.org/10.1126/science.133.3465.1702>.
- Crowson, R.A., Showers, W.J., Wright, E.K., and Hoering, T.C. (1991). Preparation of phosphate samples for oxygen isotope analysis. *Analytical Chemistry*, 63: 2397–2400.
- Dansgaard, W. (1964). Stable isotopes in precipitation. *Tellus*, 16: 436–468. <https://doi.org/10.3402/tellusa.v16i4.8993>.
- Dettman, D.L., Kohn, M.J., Quade, J., Ryerson, F.J., Ojha, T.P., and Hamidullah, S. (2001). Seasonal stable isotope evidence for a strong Asian monsoon throughout the past 10, 7 m.y. *Geology*, 29(1): 31–34. [https://doi.org/10.1130/0091-7613\(2001\)029<0031:SSIEFA>2.0.CO;2](https://doi.org/10.1130/0091-7613(2001)029<0031:SSIEFA>2.0.CO;2).
- Garvie-Lok, S.J., Varney, T.L., and Katzenberg, M.A. (2004). Preparation of bone carbonate for stable isotope analysis: the effects of treatment time and acid concentration. *Journal of Archaeological Science*, 31: 763–776. <https://doi.org/10.1016/j.jas.2003.10.014>.
- Gehler, A., Tütken, T., and Pack, A. (2011). Triple oxygen isotope analysis of bioapatite as tracer for diagenetic alteration of bones and teeth. *Palaeogeography, Palaeoclimatology, Palaeoecology*, 310: 84–91. <https://doi.org/10.1016/j.palaeo.2011.04.014>.
- Grimes, V. and Pellegrini, M. (2013). A comparison of pretreatment methods for the analysis of phosphate oxygen isotope ratios in bio-apatite. *Rapid Communications in Mass Spectrometry*, 27: 375–390. <https://doi.org/10.1002/rcm.6463>.
- Iacumin, P., Bocherens, H., Mariotti, A., and Longinelli, A. (1996). Oxygen isotope analyses of co-existing carbonate and phosphate in biogenic apatite: a way to monitor diagenetic alteration of bone phosphate? *Earth and Planetary Science Letters*, 142: 1–6. [https://doi.org/10.1016/0012-821X\(96\)00093-3](https://doi.org/10.1016/0012-821X(96)00093-3).
- Iacumin, P. and Venturelli, G. (2015). *The $\delta^{18}\text{O}$ of phosphate of ancient human biogenic apatite can really be used for quantitative palaeoclimate reconstruction?* *European Scientific Journal*, 11: 1857–7881.
- Keenan, S.W. (2016). From bone to fossil: a review of the diagenesis of bioapatite. *American Mineralogist*, 101: 1943–1951. <https://doi.org/10.2138/am-2016-5737>.
- Kock, S.T., Schitteck, K., Wissel, H., Vos, H., Ohlendorf, C., Schäbitz, F., Lupo, L.C., Kulemeyer, J.J., and Lücke, A. (2019). Stable oxygen isotope records ($\delta^{18}\text{O}$) of a high-andean cushion peatland in nw Argentina (24° S) imply South American summer monsoon related moisture changes during the late holocene. *Frontiers in Earth Science*, 7: 1–18. <https://doi.org/10.3389/feart.2019.00045>.
- Kocsis, L. (2011). Geochemical compositions of marine fossils as proxies for reconstructing ancient environmental conditions. *International Journal of Chemistry*, 65: 787–791. <https://doi.org/10.2533/chimia.2011.787>.
- Kohn, M.J. and Cerling, T.E. (2002). Stable isotope compositions of biological apatite. *Reviews in Mineralogy and Geochemistry*, 48: 455–488. <https://doi.org/10.2138/rmg.2002.48.12>.
- Kohn, M.J., Schoeninger, M.J., and Barker, W.W. (1999). Altered states: effects of diagenesis on fossil tooth chemistry. *Geochimica et Cosmochimica Acta*, 63: 2737–2747. [https://doi.org/10.1016/S0016-7037\(99\)00208-2](https://doi.org/10.1016/S0016-7037(99)00208-2).
- LaPorte, D.F., Holmden, C., Patterson, W.P., Prokopiuk, T., and Eglinton, B.M. (2009). Oxygen isotope analysis of phosphate: improved precision using TC/EA CF-IRMS. *Journal of Mass Spectrometry*, 44: 879–890. <https://doi.org/10.1002/jms.1549>.
- Lécuyer, C. (2004). Oxygen isotope analysis of phosphate. *Handbook of Stable Isotope Analytical Techniques*: 482–496. <https://doi.org/10.1016/B978-044451114-0/50024-7>.
- Lécuyer, C., Fourel, F., Seris, M., Amiot, R., Goedert, J., and Simon, L. (2019). Synthesis of in-house produced calibrated silver phosphate with a large range of oxygen isotope compositions. *Geostandards and Geoanalytical Research*, 43: 681–688. <https://doi.org/10.1111/ggr.12285>.
- Lécuyer, C., Grandjean, P., O'Neil, J.R., Cappetta, H., and Martineau, F. (1993). Thermal excursions in the ocean at the Cretaceous-Tertiary boundary (northern Morocco): $\delta^{18}\text{O}$ record of phosphatic fish debris. *Palaeogeography, Palaeoclimatology, Palaeoecology*, 105: 235–243. [https://doi.org/10.1016/0031-0182\(93\)90085-W](https://doi.org/10.1016/0031-0182(93)90085-W).
- Liu, Y., Wang, J., Chen, J., Zhang, R., Ji, Y., and Jin, Z. (2019). Pretreatment method for the analysis of phosphate oxygen isotope ($\delta^{18}\text{O}_\text{p}$) of different phosphorus fractions in freshwater sediments. *Science of the Total Environment*, 685: 229–238. <https://doi.org/10.1016/j.scitotenv.2019.05.238>.
- Longinelli, A. (1984). Oxygen isotopes in mammal bone phosphate: a new tool for paleohydrological and paleoclimatological research? *Geochimica et Cosmochimica Acta*, 48: 385–390. [https://doi.org/10.1016/0016-7037\(84\)90259-X](https://doi.org/10.1016/0016-7037(84)90259-X).
- Luz, B. and Kolodny, Y. (1985). Oxygen isotope variations in phosphate of biogenic apatites, IV. Mammal teeth and bones. *Earth and Planetary Science Letters*, 75: 29–36. [https://doi.org/10.1016/0012-821X\(85\)90047-0](https://doi.org/10.1016/0012-821X(85)90047-0).
- Luz, B., Kolodny, Y., and Horowitz, M. (1984). Fractionation of oxygen isotopes between mammalian bone-phosphate and environmental drinking water. *Geochimica et Cosmochimica Acta*, 48: 1689–1693. [https://doi.org/10.1016/0016-7037\(84\)90338-7](https://doi.org/10.1016/0016-7037(84)90338-7).
- Mine, A.H., Waldeck, A., Olack, G., Hoerner, M.E., Alex, S., and Colman, A.S. (2017). Microprecipitation and $\delta^{18}\text{O}$ analysis of



- phosphate for paleoclimate and biogeochemistry research. *Chemical Geology*, 460: 1–14. <https://doi.org/10.1016/j.chemgeo.2017.03.032>.
- O'Neil, J.R., Roe, L.J., Reinhard, E., and Blake, R.E. (1994). A rapid and precise method of oxygen isotope analysis of biogenic phosphate. *Israel Journal of Earth Sciences*, 43: 203.
- Olszta, M.J., Cheng, X., Jee, S.S., Kumar, R., Kim, Y.Y., Kaufman, M.J., Douglas, E.P., and Gower, L.B. (2007). Bone structure and formation: a new perspective. *Materials Science and Engineering: R: Reports*, 58: 77–116. <https://doi.org/10.1016/j.mser.2007.05.001>.
- Pasero, M., Kampf, A.R., Ferraris, C., Pekov, I. V., Rakovan, J., and White, T.J. (2010). Nomenclature of the apatite supergroup minerals. *European Journal of Mineralogy*, 22: 163–179. <https://doi.org/10.1127/0935-1221/2010/0022-2022>.
- Pederzani, S., Snoeck, C., Wacker, U., and Britton, K. (2020). Anion exchange resin and slow precipitation preclude the need for pretreatments in silver phosphate preparation for oxygen isotope analysis of bioapatites. *Chemical Geology*, 534: 119455.
- Pellegrini, M. and Snoeck, C. (2016). Comparing bioapatite carbonate pre-treatments for isotopic measurements: Part 2 - impact on carbon and oxygen isotope compositions. *Chemical Geology*, 420: 88–96. <https://doi.org/10.1016/j.chemgeo.2015.10.038>.
- Puc at, E., Joachimski, M.M., Bouilloux, A., Monna, F., Bonin, A., Motreuil, S., Morini ere, P., H enard, S., Mourin, J., Dera, G., and Quesne, D. (2010). Revised phosphate-water fractionation equation reassessing paleotemperatures derived from biogenic apatite. *Earth and Planetary Science Letters*, 298: 135–142. <https://doi.org/10.1016/j.epsl.2010.07.034>.
- Rozanski, K., Aragu as-Aragu as, L., and Gonfiantini, R. (1993). Isotopic patterns in modern global precipitation. *Geophysical Monograph Series*, 78: 1–36. <https://doi.org/10.1029/gm078p0001>.
- Sharp, Z.D., Atudorei, V., and Furrer, H. (2000). The effect of diagenesis on oxygen isotope ratios of biogenic phosphates. *American Journal of Science*, 300: 222–237.
- Snoeck, C. and Pellegrini, M. (2015). Comparing bioapatite carbonate pre-treatments for isotopic measurements: Part 1- Impact on structure and chemical composition. *Chemical Geology*, 417: 394–403. <https://doi.org/10.1016/j.chemgeo.2015.10.004>.
- Steiger, N.J., Steig, E.J., Dee, S.G., Roe, G.H., and Hakim, G.J. (2017). Climate reconstruction using data assimilation of water isotope ratios from ice cores. *Journal of Geophysical Research: Atmospheres*: 1545–1568. <https://doi.org/10.1002/2016JD026011>.
- Szab o, P., Kocsis, L., Vennemann, T., Pandolfi, L., Kov acs, J., Martinetto, E., and Dem eny, A. (2017). Pliocene–Early Pleistocene climatic trends in the Italian Peninsula based on stable oxygen and carbon isotope compositions of rhinoceros and gomphothere tooth enamel. *Quaternary Science Reviews*, 157: 52–65. <https://doi.org/10.1016/j.quascirev.2016.11.003>.
- Tudge, A.P. (1960). A method of analysis of oxygen isotopes in orthophosphate-its use in the measurement of paleotemperatures. *Geochimica et Cosmochimica Acta*, 18: 81–93. [https://doi.org/10.1016/0016-7037\(60\)90019-3](https://doi.org/10.1016/0016-7037(60)90019-3).
- Vennemann, T.W., Fricke, H., Blake, R.E., O'Neil, J.R., and Colman, A. (2002). Oxygen isotope analysis of phosphates: a comparison of techniques for analysis of Oxygen isotope analysis of phosphates: a comparison of techniques. *Chemical Geology*, 185: 321–336.
- Vodila, G., Palcsu, L., Fut o, I., and Sz ant o, Z. (2011). A 9-year record of stable isotope ratios of precipitation in Eastern Hungary: implications on isotope hydrology and regional palaeoclimatology. *Journal of Hydrology*, 400: 144–153. <https://doi.org/10.1016/j.jhydrol.2011.01.030>.
- White, C., Longsta, F.J., and Law, K.R. (2004). Exploring the effects of environment, physiology and diet on oxygen isotope ratios in ancient Nubian bones and teeth. *Journal of Archaeological Science*, 31: 233–250. <https://doi.org/10.1016/j.jas.2003.08.007>.
- Wopenka, B. and Pasteris, J.D. (2005). A mineralogical perspective on the apatite in bone. *Materials Science and Engineering: C*, 25: 131–143. <https://doi.org/10.1016/j.msec.2005.01.008>.
- Xu, C., Buckley, B.M., Wang, S.S., An, W., Li, Z., Nakatsuka, T., and Guo, Z. (2021). Oxygen isotopes in tree rings from Greenland: a new proxy of NAO. *Atmosphere*, 12: 39. <https://doi.org/10.3390/atmos12010039>.
- Zazzo, A., L ecuyer, C., and Mariotti, A. (2004). Experimentally-controlled carbon and oxygen isotope exchange between bioapatites and water under inorganic and microbially-mediated conditions. *Geochimica et Cosmochimica Acta*, 68: 1–12. [https://doi.org/10.1016/S0016-7037\(03\)00278-3](https://doi.org/10.1016/S0016-7037(03)00278-3).



APPENDIX

Table 1. The average $\delta^{18}\text{O}$ values of the NE-6H batch, including standard deviations and the calculated differences from the previously-measured data. The average mass changes after several pre-cleaning procedures, compared to the original masses; the yield and the differences from the known values (Szabó et al., 2017) weighted with the standard deviation squared are also indicated

$\delta^{18}\text{O}_{\text{PO}_4}$ [‰, V-SMOW] values of NE-6H batch					Average mass difference after pre-cleaning [%]	Yield [%]
No. of sample	Prev. measured	Average	s	Difference (D)		
1	18.9	18.9	0.08	0.06	95.4	65.1
2	18.5	18.4	0.01	−0.10	100.8	74.7
3	20.2	19.0	0.14	−1.12	101.7	78.1
4	14.7	15.5	0.05	0.85	99.2	72.5
5	14.5	14.9	0.47	0.41	98.7	73.9
6	15.1	15.3	0.19	0.13	99.5	63.0
7	13.2	13.9	0.17	0.75	99.8	73.4
8	11.9	12.7	0.11	0.76	101.3	70.1
9	14.2	14.5	0.09	0.29	100.6	72.2
10	16.7	16.8	0.34	0.14	96.6	69.0
ΣD^2				3.41		
$\Sigma(D^2 \times s^2)$				0.09		
average mass difference [%]					99.4	
average yield [%]						71.2

Table 2. The average $\delta^{18}\text{O}$ values of the NE-24H batch, including the standard deviations and the calculated differences from the previously-measured data. The average mass changes after several pre-cleaning procedures, compared to the original masses; the yield and the differences from the known values (Szabó et al., 2017) weighted with the standard deviation squared are also indicated

$\delta^{18}\text{O}_{\text{PO}_4}$ [‰, V-SMOW] values of NE-24H batch					Average mass difference after pre-cleaning [%]	Yield [%]
No. of sample	Prev. measured	Average	s	Difference (D)		
1	18.9	19.9	0.12	1.00	105.6	77.3
2	18.5	19.5	0.30	0.99	102.9	74.5
3	20.2	20.1	0.31	−0.05	101.5	77.0
4	14.7	16.1	0.21	1.44	99.2	72.9
5	14.5	15.6	0.06	1.12	91.9	65.1
6	15.1	16.0	0.24	0.86	98.2	59.0
7	13.2	14.7	0.36	1.55	99.3	76.9
8	11.9	12.9	0.21	0.96	98.3	71.3
9	14.2	15.6	0.05	1.39	101.9	71.7
10	16.7	17.8	0.09	1.10	98.3	69.1
ΣD^2				12.48		
$\Sigma(D^2 \times s^2)$				0.60		
average mass difference [%]					99.7	
average yield [%]						71.5

Table 3. The average $\delta^{18}\text{O}$ values of the A-6H batch, including the standard deviations and the calculated differences from the previously-measured data. The average mass changes after several pre-cleaning procedures, compared to the original masses; the yield and the differences from the known values (Szabó et al., 2017) weighted with the standard deviation squared are also indicated

$\delta^{18}\text{O}_{\text{PO}_4}$ [‰, V-SMOW] values of A-6H batch					Average mass difference after pre-cleaning [%]	Yield [%]
No. of sample	Prev. measured	Average	s	Difference (D)		
1	18.9	19.1	0.37	0.18	84.6	62.4
2	18.5	19.0	0.40	0.51	86.7	66.0
3	20.2	19.7	0.22	−0.50	86.4	69.6
4	14.7	15.8	0.04	1.14	88.4	66.4
5	14.5	15.6	0.05	1.08	78.7	57.8
6	15.1	16.1	0.06	1.02	76.9	51.3

(continued)



Table 3. Continued

$\delta^{18}\text{O}_{\text{PO}_4}$ [‰, V-SMOW] values of A-6H batch					Average mass difference after pre-cleaning [%]	Yield [%]
No. of sample	Prev. measured	Average	s	Difference (D)		
7	13.2	14.5	0.17	1.36	82.1	60.6
8	11.9	13.0	0.15	1.09	84.9	81.5
9	14.2	15.1	0.16	0.91	83.4	62.9
10	16.7	17.3	0.22	0.61	69.9	48.0
ΣD^2				8.27		
$\Sigma(D^2 \times s^2)$				0.19		
average mass difference [%]					82.2	
average yield [%]						62.6

Table 4. The average $\delta^{18}\text{O}$ values of the A-24H batch, including the standard deviations and the calculated differences from the previously-measured data. The average mass changes after several pre-cleaning procedures, compared to the original masses; the yield and the differences from the known values (Szabó et al., 2017) weighted with the standard deviation squared are also indicated

$\delta^{18}\text{O}_{\text{PO}_4}$ [‰, V-SMOW] values of A-24H batch					Average mass difference after pre-cleaning [%]	Yield [%]
No. of sample	Prev. measured	Average	s	Difference (D)		
1	18.9	18.7	0.49	-0.14	93.6	66.2
2	18.5	18.3	0.30	-0.26	93.3	69.8
3	20.2	19.6	0.38	-0.60	95.4	73.3
4	14.7	15.2	0.43	0.57	90.1	67.1
5	14.5	16.0	0.50	1.50	90.1	63.9
6	15.1	16.0	0.23	0.88	90.5	48.4
7	13.2	14.7	0.22	1.52	87.7	65.4
8	11.9	13.0	0.39	1.07	88.8	66.6
9	14.2	15.2	0.61	0.98	91.8	67.2
10	16.7	17.4	0.13	0.69	84.7	57.8
ΣD^2				8.71		
$\Sigma(D^2 \times s^2)$				1.38		
average mass difference [%]					90.6	
average yield [%]						64.6

Table 5. The average $\delta^{18}\text{O}$ values of the PA-6H batch, including the standard deviations and the calculated differences from the previously-measured data. The average mass changes after several pre-cleaning procedures, compared to the original masses; the yield and the differences from the known values (Szabó et al., 2017) weighted with the standard deviation squared are also indicated

$\delta^{18}\text{O}_{\text{PO}_4}$ [‰, V-SMOW] values of PA-6H batch					Average mass difference after pre-cleaning [%]	Yield [%]
No. of sample	Prev. measured	Average	s	Difference (D)		
1	18.9	16.5	0.33	-2.35	90.5	67.2
2	18.5	17.0	0.21	-1.52	90.6	68.1
3	20.2	18.8	0.63	-1.36	92.2	67.2
4	14.7	15.6	0.69	0.97	82.1	60.1
5	14.5	16.0	0.71	1.47	77.4	53.2
6	15.1	16.0	1.09	0.91	70.7	45.5
7	13.2	15.0	0.80	1.83	79.3	60.0
8	11.9	14.6	0.42	2.70	83.8	61.6
9	14.2	15.9	0.91	1.68	83.2	61.6
10	16.7	17.7	0.34	1.06	69.4	49.7
ΣD^2				28.21		
$\Sigma(D^2 \times s^2)$				9.86		
average mass difference [%]					81.9	
average yield [%]						59.4



Table 6. The average $\delta^{18}\text{O}$ values of the PA-24H batch, including the standard deviations and the calculated differences from the previously-measured data. The average mass changes after several pre-cleaning procedures, compared to the original masses; the yield and the differences from the known values (Szabó et al., 2017) weighted with the standard deviation squared are also indicated

$\delta^{18}\text{O}_{\text{PO}_4}$ [‰, V-SMOW] values of PA-24H batch					Average mass difference after pre-cleaning [%]	Yield [%]
No. of sample	Prev. measured	Average	s	Difference (D)		
1	18.9	19.6	0.20	0.68	93.8	67.4
2	18.5	19.5	0.30	1.00	93.6	72.5
3	20.2	20.1	0.28	-0.07	95.1	71.7
4	14.7	16.7	0.31	2.06	85.7	63.4
5	14.5	16.3	0.42	1.78	76.7	56.3
6	15.1	16.5	0.24	1.34	76.7	49.3
7	13.2	14.9	0.46	1.72	87.4	63.2
8	11.9	14.3	0.64	2.36	88.8	66.2
9	14.2	15.3	0.25	1.06	89.1	65.6
10	16.7	16.9	0.72	0.21	72.9	50.2
ΣD^2				20.41		
$\Sigma(D^2 \times s^2)$				4.22		
average mass difference [%]					86.0	
average yield [%]						62.6

Table 7. The average $\delta^{18}\text{O}$ values of the HCA-6H batch, including the standard deviations and the calculated differences from the previously-measured data. The average mass changes after several pre-cleaning procedures, compared to the original masses; the yield and the differences from the known values (Szabó et al., 2017) weighted with the standard deviation squared are also indicated

$\delta^{18}\text{O}_{\text{PO}_4}$ [‰, V-SMOW] values of HCA-6H batch					Average mass difference after pre-cleaning [%]	Yield [%]
No. of sample	Prev. measured	Average	s	Difference (D)		
1	18.9	16.9	0.61	-1.96	80.2	70.3
2	18.5	16.7	0.83	-1.80	67.9	56.3
3	20.2	19.3	0.48	-0.91	73.2	63.3
4	14.7	16.5	0.58	1.86	73.1	54.7
5	14.5	17.0	0.38	2.55	69.5	58.0
6	15.1	16.5	0.86	1.42	63.4	51.3
7	13.2	15.4	0.84	2.27	72.3	60.7
8	11.9	11.7	0.10	-0.24	72.3	60.0
9	14.2	12.9	0.33	-1.28	59.7	62.5
10	16.7	14.9	0.68	-1.80	59.0	50.7
ΣD^2				29.97		
$\Sigma(D^2 \times s^2)$				12.82		
average mass difference [%]					69.1	
average yield [%]						58.8

Table 8. The average $\delta^{18}\text{O}$ values of the HCA-24H batch, including the standard deviations and the calculated differences from the previously-measured data. The average mass changes after several pre-cleaning procedures, compared to the original masses; the yield and the differences from the known values (Szabó et al., 2017) weighted with the standard deviation squared are also indicated

$\delta^{18}\text{O}_{\text{PO}_4}$ [‰, V-SMOW] values of HCA-24H batch					Average mass difference after pre-cleaning [%]	Yield [%]
No. of sample	Prev. measured	Average	s	Difference (D)		
1	18.9	18.2	0.18	-0.70	73.0	67.5
2	18.5	18.9	0.80	0.36	69.8	71.4
3	20.2	19.8	0.36	-0.36	75.2	65.8
4	14.7	15.9	0.57	1.23	70.2	58.3
5	14.5	16.3	0.92	1.77	59.5	57.2
6	15.1	15.7	0.22	0.56	61.7	51.2

(continued)



Table 8. Continued

$\delta^{18}\text{O}_{\text{PO}_4}$ [‰, V-SMOW] values of HCA-24H batch					Average mass difference after pre-cleaning [%]	Yield [%]
No. of sample	Prev. measured	Average	s	Difference (D)		
7	13.2	14.6	0.46	1.47	68.9	57.6
8	11.9	13.3	0.46	1.36	72.4	60.4
9	14.2	14.9	0.08	0.68	63.1	64.5
10	16.7	17.6	0.49	0.91	52.9	45.3
ΣD^2				11.01		
$\Sigma(D^2 \times s^2)$				4.29		
average mass difference [%]					66.7	
average yield [%]						59.9

Open Access statement. This is an open-access article distributed under the terms of the Creative Commons Attribution 4.0 International License (<https://creativecommons.org/licenses/by/4.0/>), which permits unrestricted use, distribution, and reproduction in any medium, provided the original author and source are credited, a link to the CC License is provided, and changes – if any – are indicated. (SID_1)

